

# Physico-Chemical Characterization of Soymilk Particles as a Function of Their Volume Fraction: Comparison with Theoretical Systems

Elise Ringgenberg · Milena Corredig ·  
Marcela Alexander

Received: 1 September 2011 / Accepted: 30 May 2012 / Published online: 13 June 2012  
© Springer Science+Business Media, LLC 2012

**Abstract** The physico-chemical properties of soymilk particles were investigated as a function of concentration of protein in soymilk. Soymilk samples were prepared using different water-to-protein ratios, resulting in 4 %, 5 % and 7 % protein content. The soymilk particles were not significantly different in their protein composition, surface hydrophobicity and intrinsic fluorescence; however, their  $\zeta$ -potential and particle size were affected by protein concentration. Using a relation between the effective refractive index of soymilk and the turbidity parameter determined experimentally using diffusing wave spectroscopy, it was possible to estimate, for the first time, a voluminosity of 4.11 mL/g and a refractive index of 1.388 for the colloidal particles. This allowed conversion of protein content to volume fraction, and comparison of the experimental data collected by diffusing wave spectroscopy, rheology and ultrasonic spectroscopy with theoretical models.

**Keywords** Soy-milk · Physico-chemical characterization · Voluminosity · Diffusing wave spectroscopy · Ultrasound

## Introduction

Consumers in western countries are increasingly seeking food products that offer added health benefits, in part due to an increased awareness of the effects of diet on health. Over the past two decades, research has shown strong evidence for the potential use of soy in the prevention of chronic diseases, which has positively affected soymilk

and soy-foods consumption.<sup>1–3</sup> To meet this growing demand, food companies are faced with new challenges to formulate innovative products that provide added health benefits. One of the possible ways to achieve this would be to exploit the use of soymilk as an ingredient base in foods and beverage products; however, a better understanding of the fundamental colloidal characteristics of soymilk is required to succeed.

Soymilk particles are colloidal assemblies derived from the aqueous extraction of soybeans and are made up of various components, including lipids (such as triglycerides and phospholipids), proteins, complex carbohydrates, minerals and phytates.<sup>4,5</sup> There are two major proteins in soymilk, namely glycinin and  $\beta$ -conglycinin, constituting about 40 % and 30 % of total soy protein, respectively. Research on the chemical nature of soymilk particles revealed that they are composed of all the major subunits present in the original storage protein in the seed.<sup>5–7</sup>

Heat treatment of soymilk is necessary to denature antinutritional components, prolong shelf-life and stability, as well as to improve sensorial characteristics of the final product.<sup>8–10</sup> Several studies report that heat treatment is essential to achieve colloidal stability of soymilk.<sup>8,11</sup> Protein particles are formed during heating through disruption, and subsequent rearrangement and aggregation of the storage proteins present in the seed.<sup>4–6,12–16</sup> Heat treatment was found to decrease the fraction of large particles, defined as particles larger than 100 nm (by differential centrifugation), and increase the fraction of medium-sized particles, defined as particles between 40 nm and 100 nm, which form by association of supernatant proteins with each other. The increase in medium sized particles seemed to be responsible for the colloidal stability of the system.<sup>5,6,14</sup> In agreement, another study reported that soymilk particles after heat-treatment are polydisperse in size with an average particle diameter of around  $0.20 \pm 0.01 \mu\text{m}$ .<sup>5</sup>

E. Ringgenberg · M. Corredig · M. Alexander (✉)  
Department of Food Science, University of Guelph,  
Guelph, Ontario N1G 2W1, Canada  
e-mail: maalexan@uoguelph.ca

Research has been conducted on the behaviour and bulk properties of soymilk undergoing various processing methods such as heating, homogenization and high-pressure treatment, to identify ideal processing conditions<sup>4,8,10,17–19</sup> as well as the structural characteristics of soymilk particles such as size, composition, chemical nature of inter-particle bonds and the general physico-chemical characteristics.<sup>5,7,14,20</sup> However, very little is known on the physical nature of soymilk particles, and if their behaviour can be somewhat predicted by using established theoretical models of colloidal science.

Knowing that soymilk particles are formed through the disruption and subsequent rearrangement and aggregation of soy protein subunits during heat treatment, this work investigates the dependence (if any) of the physical characteristics of the ensuing soymilk particles after this disruption and rearrangement process as a function of water-to-bean ratio. Whether an effect on the nature of the particles is observed presents important implications in terms of the colloidal and processing behaviour of soymilk. The comparison of physical properties of soymilk particles made from different water-to-bean ratios was investigated, such as size, surface hydrophobicity, intrinsic fluorescence,  $\zeta$ -potential. Furthermore, the mass-to-volume conversion factor of the soymilk particles was calculated, allowing for a comparison between experimental results and theoretical models. As a corollary, the index of refraction of the soymilk particle was estimated.

## Materials and Methods

### Soymilk Preparation

Soybean seeds (Harovinton variety) were obtained from the Greenhouse and Processing Crops Research Centre of Agriculture and Agri-Food Canada (Harrow, Ontario). All chemicals used in this work were purchased from Sigma Chemical (St Louis, MO, USA) or at Fisher Scientific (Mississauga, ON, Canada). Ultrapure water was used for the preparation of soymilk (Milli-Q Integral Pure and Ultrapure water systems, Billerica Massachusetts).

Soymilk was prepared as previously described<sup>5</sup> with slight modifications. Three stock batches of soymilk were prepared with varying protein concentration (4, 5 and 7 %), using three ratios of water to soybeans (based on protein): 22:1, 18:1 and 12:1, respectively. The soybeans used had 43.5 % protein (as determined by Grainspec near infra-red spectroscopy).

Soybeans were weighed and soaked overnight for 12–18 h, at room temperature in ultrapure water. Once soaked, the soybeans were rinsed and drained with cold water several times, then reweighed to determine the amount of water absorbed by the beans. The amount of water to be added to

the soaked beans before blending was determined by correcting for the amount of absorbed water:

$$Ax(W_{db}xC_p) - (W_{db} - W_{wb}) = g(\text{water}) \quad (1)$$

where A is the desired ratio of water-to-protein,  $W_{db}$  is the weight of dry beans,  $W_{wb}$  is the weight of wet beans and  $C_p$  is the original concentration of protein in the bean. Of the water to be added to the soaked beans, about half was added at room temperature (23 °C) and blended with the beans (commercial blender, WARING, New Hartford, CT) at high speed for 3.5 min. The remaining water was heated to 60 °C and added to the slurry to enhance protein extraction. This mixture was blended for an additional 30 s at high speed. The slurry was passed through a juice extractor (Juiceman, professional series 211, Korea) to remove coarse material (okara, which is mainly composed of insoluble fibre material), and was then passed through the juice extractor a second time. The soymilk obtained was further filtered through a cheese cloth.

Soymilk was transferred into 20 mL test tubes and placed in a water bath set at 95 °C. After heating for 7 min, the tubes were then immediately cooled to room temperature in an ice-water bath. To further remove residual fiber and large particles,<sup>5</sup> the soymilk was centrifuged at 8000 g for 30 min at 20 °C (Optima LE-80 K Beckman Coulter, CA, USA) and filtered through cellulose paper filters (25  $\mu\text{m}$ , Fisherbrand, Fisher Scientific).

Soymilk serum was obtained by ultrafiltration using centrifugal microfilters (10 mL Macrosep 10 K Omega, Pall Corporation, NY, USA), by centrifuging at 5000 g for 2 h (Beckman Coulter, J2-21, CA, USA). The ionic composition of the serum was analyzed by atomic absorption spectroscopy by Laboratory Services, Agriculture and Food Laboratory, Guelph, Ontario.

### Determination of Total Solids and Protein Concentration

The total solids content was determined using a forced air oven method, by placing the samples in dry aluminum dishes containing dried sea-sand as a dispersing agent (Fisher Scientific), and drying at 105 °C until constant weight.

Protein was determined using a modified Lowry assay method, according to manufacturer's instructions (DC Protein Assay, Bio-Rad, Hercules, CA). Bovine Serum Albumin (Thermo Scientific, Rockford, USA) was used as the standard.

### Particle Protein Content and Composition

Previous research revealed that over 50 % of proteins in soymilk are present as medium and large size particles (>40 nm) while the rest is present as supernatant particles

(<40 nm).<sup>14</sup> Other studies showed that the average particle size of soymilk and defatted soymilk is roughly between 40 nm and 200 nm.<sup>5,7</sup> In order to take a closer look at soymilk particles (>40 nm), 4 and 7 % protein soymilk samples were centrifuged at 100,000 g for 30 min at 20 °C. The pellet obtained from centrifugation at 100,000 g (soymilk particles) was resuspended in 0.1 M phosphate buffer (pH 8) using an UltraTurrax dispersing unit (PowerGen 125, Fisher Scientific) for 90 s. After resuspension in buffer, samples were centrifuged further at 20,000 g for 30 min at 20 °C in order to further “clean up” the soy-milk. The obtained supernatant will be referred to as “supernatant after 20,000 g” in the remainder of the manuscript. Both pellets and supernatants (obtained after the two centrifugations) were analyzed in terms of total solids and protein content by means of mass-balance calculations. Total solids were measured by the drying oven method as described above, while the protein content was determined by the DUMAS method, using a Nitrogen Analyzer (LECO, FP-528, Mississauga, ON, Canada). EDTA was used as a standard for calibration and the conversion factor used was 6.25.

#### Refractometry

The refractive index of soymilk at different dilutions was recorded at room temperature using a Carl Zeiss refractometer (Model 74108, Germany). Soymilk batches (4, 5 and 7 % protein) were diluted in series with their respective serums prepared by ultrafiltration. Six dilutions were made per batch, down to a dilution of 60:40 soymilk-to-serum (v/v). For each dilution, the amount of protein was determined using the modified Lowry method (see above). Results were obtained for triplicate soymilk batches. The refractive index of the serum was measured for each soymilk batch. Ultrapure water was used as the reference, with a measured refractive index of 1.333 at 25 °C.

#### Gel Electrophoresis

Sodium Dodecyl Sulfate-Polyacrylamide Gel Electrophoresis (SDS-PAGE) was carried out on the “supernatant after 20,000 g” (as described above) of 4 % and 7 % protein soymilk.

Extraction buffer (50 mM Tris-HCl, 5 M urea, 1% SDS, and 4 % 2-mercaptoethanol, pH 8.0) was added to soymilk samples in varying amounts depending on the initial sample protein concentration, and the mixture was incubated for 1 h at room temperature. Electrophoresis buffer (200 µL) (125 mM Tris-HCl, 5 M urea, 1 % SDS, 20 % glycerol, 4 % 2-mercaptoethanol, and 1 % bromophenol blue, pH 6.8) was then added to each sample, to bring the final volume to 600 µL. The final protein concentration in these sample mixtures was 0.286 g/100 mL. The solutions were heated

at 95 °C for 5 min and centrifuged at 6,000 g for 10 min using an Eppendorf centrifuge (Brinkmann Instruments, Westbury, NY). Sample aliquots of 6 µL were loaded into a 12.5 % acrylamide running gel with a 4 % stacking gel in Bio-Rad mini-protein electrophoresis unit (Bio-Rad Laboratories, Hercules, CA), at a constant voltage of 175 V. Molecular weight standards were loaded in 10 µL aliquots (BIO-RAD Molecular Weight Standards, Low Range, BIO-RAD Laboratories, Hercules, USA). Gels were then stained with Coomassie blue R-250 stain solution and destained according to manufacturer’s instructions. The protein bands were analyzed using image analysis software (Image-Master® 1D, version 2.0, Amersham Biosciences) and scanned using a SHARP JX-330 scanner (Amersham Biosciences, Quebec, Canada).

#### Fluorescence Measurements

The fluorescence spectrum of the protein present in the 4 % and 7 % soymilk samples was measured using a Shimadzu RF-5301 PC spectrofluorophotometer (Mandel Scientific, Guelph, Canada), using 280 nm as excitation wavelength, with excitation and emission slots of 5 nm. Samples were prepared by diluting soymilk in 30 mM phosphate buffer (pH 7) to a final concentration of 20 µg/mL. The fluorescence spectrum was collected at 300–400 nm.

Surface hydrophobicity of the protein complexes was determined using 1-anilino-8-naphthalene sulfonate (ANS). Titrations were carried out using a Mandel Spectrofluorophotometer (RF-5301 PC, Shimadzu, North America) on soymilk samples containing 4 and 7 % protein. The samples were diluted in 30 mM phosphate buffer (pH 7) to a final protein concentration of 50 µg/mL, and ANS was added incrementally in a range of concentration from 0.003 mM to 0.25 mM. Excitation was set at 390 nm and the fluorescence spectrum (400–650 nm) was measured, with bandwidths of 5 nm. The intensity at the maximum peak of emission (470 nm) was then measured at each ANS concentration. Sigmaplot Enzyme Kinetics 1.3 was used to fit the plot to the Michaelis-Menten model (single substrate binding model), from which the apparent dissociation constant of the protein-ANS complex ( $K_d^{app}$ ) and the overall binding capacity  $F_{max}$  was measured. The ratio  $F_{max}/K_d^{app}$  was also calculated, which gives an estimate of protein surface hydrophobicity index (PSH), which takes into account the affinity and the number of hydrophobic sites.<sup>21</sup>

#### Light Scattering Measurements

Dynamic light scattering (DLS) was employed to determine the average hydrodynamic size and  $\zeta$ -potential of the soymilk particles. For size measurements, soymilk samples were diluted ~10,000 times in filtered phosphate buffer

(pore size 0.22  $\mu\text{m}$ ) at pH 8.0,<sup>7</sup> and placed in a Zetasizer Nanoseries (Nano ZS, Malvern Instruments, Worcestershire, UK). The cuvettes were pre-rinsed with filtered buffer prior to adding the sample to ensure no dust or other particulates were present.  $\zeta$ -potential measurements were also performed with the Zetasizer, diluting the soymilk samples ~5000 times with their respective stock-derived serums, using DTS1060C clear disposable zeta cells (Malvern Instruments).

Since the measurements described above required the samples to be highly diluted, diffusing wave spectroscopy (DWS) was also employed, as this technique does not require dilution of soymilk. It was then possible to measure the hydrodynamic size and turbidity parameter of the soymilk particles as a function of the concentration of protein present. The dilutions were made for all three batches of soymilk dispersed in their own respective serum (as prepared by ultrafiltration, see above).

The DWS equipment consisted of passing a monochromatic variable power Verdi V-2 pumped Nd:YAG laser (Coherent Inc., Santa Clara, CA) emitting at 532 nm and power of 300 mW (Coherent, Santa Clara, CA, USA), through the sample. The sample (~2 mL) was contained in a glass cuvette with a path length of 5 mm (Hellma Canada Limited, Concord, Canada). A water bath was used to maintain sample temperature at 23 °C. A detailed description of the setup can be found elsewhere.<sup>22</sup> Calibration of the laser intensity was performed daily and used to calculate the turbidity ( $1/l^*$  parameter) and apparent radius of the sample particles, using specially designed software (Mediaventon Inc, Ontario, Canada).

In general, the position of particles with respect to one another will affect the angular distribution of the scattered light, giving rise to changes in turbidity, since  $1/l^*$  is a cooperative randomization of light. For completely non-interacting scatterers, only the physical and optical characteristics of the scatterers, such as refractive index contrast, size and shape (related by the form factor  $F(q)$ ) determine their scattering behavior. In concentrated systems such as those described in this work, however, the spatial correlation between the particles will also depend on the interactions between them, as given by the structure factor,  $S(q)$ . The general expression for  $l^*$  in systems with interacting particles will be then given by

$$l^* \propto \left( \int_0^{2k} F(q) S(q) q^3 dq \right)^{-1} \quad (2)$$

where  $q=2k \sin \theta/2$  is the wave vector of the light.<sup>23</sup> Therefore, changes in the  $1/l^*$  parameter can be taken as indications of changes in the organization of the colloids within the suspension (due to concentration effects, electrostatic charges, etc.) when all other

physical parameters mentioned above remain constant. Most importantly, a correlation in the positions of the particles will also play an important role in the degree of mobility of the individual particles. The dynamics of the sample will in turn be displayed in the diffusion coefficient obtained from the experimental correlation functions collected by DWS.

### Electro-Acoustic Spectroscopy

Electroacoustics also does not require sample dilution and allows in-situ investigation of particle characteristics such as  $\zeta$ -potential and size of concentrated suspensions.<sup>24,25</sup> For electroacoustic analysis, an ultrasound wave is applied to a sample, generating an electric potential, which is registered as colloidal vibration current (CVI), and can be related to dynamic electrophoretic mobility,  $\mu_d$ .<sup>25,26</sup>

$$CVI = A(\omega)F(Z)\phi \frac{\Delta\rho}{\rho_m} \mu_d \quad (3)$$

where  $A(\omega)$  is a calibration function,  $F(Z)$  is determined by the acoustic impedance of the suspension and is automatically measured by the instrument,  $\phi$  is the volume fraction of particles, and  $\Delta\rho$  is the difference in density between the particles and the suspension medium which has density  $\rho_m$ . According to this theory, the complete functional dependence of the CVI on  $\zeta$ -potential, particle size and frequency are incorporated in the dynamic mobility.

The dynamic mobility was obtained for the 4 %, 5 % and 7 % protein soymilk samples over a range of dilutions prepared using their corresponding serum. The total solids content (% w/w) was determined for each dilution using the forced-air oven drying method, as described above. The background CVI, was measured individually for each sample using the appropriate stock-derived serum. The dynamic mobility was also determined for model silica Ludox particle suspensions (AS-30, Sigma-Aldrich) of volume fractions ranging from 2.3 % to about 16.3 %.

Calibration of the equipment was performed using a 10 % w/w Ludox silica particles suspended in 10 mM KCl. Ultrasound pulses were transmitted through the sample at a constant frequency of 3 MHz. Parameters for the background medium were defined as water with the following physical characteristics: density of 0.997 g/cm<sup>3</sup> (at 25 °C), thermal conductivity of 6.065 mW/cm/C, heat capacity of 4.18 J/g/C, thermal expansion of  $2.570 \times 10^4$  1/C, sound speed of 1496.7 m/s, intrinsic attenuation at 100 MHz of 0.186 db/cm/MHz. The dispersed particles were defined as soft particles (temp, 25 °C), with the following characteristics: density of 1.2800 g/cm<sup>3</sup> (arbitrary number), thermal conductivity of 1.150 mW/cm/C, heat capacity of 1.000 J/g/C, thermal expansion of  $2.700 \times 10^4$  1/C.



## Flow Behaviour Measurements

Flow behaviour measurements were carried out with an Anton-Paar rheometer (MCR 301, Anto-Paar, Graz, Austria), using a concentric cylinder with a 1 mm gap. Soymilk samples were diluted to various protein concentrations (from ~0.01 % protein to undiluted soymilk) using ultrapure water and measurements were carried out at 23 °C. A shear ramp of 0.8–100 s<sup>-1</sup> was used. Time between measurements was increased from an initial 100 s to a final 1 s.

## Microscopy

Scanning electron microscopy (SEM) and cryo-transmission electron microscopy (TEM) were employed to observe the microstructure of the soymilk. Samples for SEM were prepared on well-polished carbon planchets sputtered with gold for 3.5 min (Emitech K550, Ashford, Kent, UK) using a self assembled monolayer technique.<sup>26,27</sup> Carbon planchets were incubated for at least 18 h into a 2 mM 11-mercapto-undecanoic acid (11-MUA) solution, diluted with 100 % ethanol to a concentration of 0.044 % to form the self-assembled monolayer. A mixed solution of chemical linkers consisting of N-hydroxysulfosuccinimide and 1-ethyl-3-(3-dimethylaminopropyl) carbodiimide was used for the protein binding. The carbon planchets were rinsed with ultrapure water and placed in the soymilk samples for 1 h, after which the soymilk was exchanged with water. The water was then replaced with 1.5 % glutaraldehyde solution (the fixing agent), and left to soak for 30 min. The carbon planchets were then rinsed by ultrapure water and subjected to critical point drying. Once dry, the carbon planchets were put in a desiccator overnight and sputter coated for 2 min with gold before taking the images. Imaging was performed with the SEM Hitachi S-570 (accelerated voltage kept at 10 kV) and viewed digitally using Quartz PCI software (Version 8, Vancouver, BC, Canada). Efforts were made to select two micrographs that best represent a total of 30 and 50 micrographs taken of the 4 and 7 % protein soymilk samples, respectively.

For CryoTEM samples, quantifoils grids with 2 µm holes, spaced 2 µm apart on 200 µm mesh copper grids, were prepared by glow-discharging using an air plasma cleaner (Harrick plasma cleaner/sterilizer PDC-32 G) for 2 min. Soymilk samples (~5 µL) were placed onto the grids, blotted two times for 2 s each, using the Vitrobot (FEI, Oregon, USA), and cryogenically frozen in liquid ethane immediately after. The samples were kept at -175 °C until use. The structure of soymilk particles was observed using a TECNAI Cryo-Transmission Electron Microscope (G2 F20, FEI, Oregon, USA).

## Statistical Analysis

All experiments were conducted at least three times. Statistical differences were calculated using general linear models where applicable, and independent sample *t*-test, using the statistical analysis program R (R Development Core Team, R Foundation for Statistical Computing, version 2.12.2. Vienna, Austria). Differences in this manuscript are significant at a level of  $p < 0.05$ .

## Results

### Characterization of the Soymilk Particles Prepared from 4 and 7 % Protein Soymilk

Due to the sensitive nature of the stability of colloidal protein aggregates to their environment, the serum in which the particles are dispersed will influence particle structure and interactions. The ionic composition of the serum obtained by ultrafiltration (see [Materials and Methods](#)) is summarized in Table 1. The two soymilk samples, prepared with the lowest and the highest water-to-bean ratio (resulting in a 7 % and 4 % final protein composition), showed different serum composition. As expected, the higher bean-to-water ratio (7 % protein soymilk) produced serum with a higher amount of ions than the 4 % protein soymilk. Accordingly, 7 % protein soymilk contained higher total solids (10.8 % w/w) compared to 4 % protein soymilk (5.9 % w/w). The increase in ion concentration was roughly double between 4 % and 7 % soymilk serum, as were the total solids between the 4 and 7 % protein soymilk samples.

Table 1 also shows the values of refractive index of the serum of both 4 % and 7 % protein soymilk, measured at 23 °C. The values were very close to the refractive index of water (1.333), giving further indication that the serum contains mostly minerals, with mono- or disaccharides or other low molecular weight substances.

The protein content of the “supernatant” (please note that this word is used here to refer to the “cleaned-up milk” obtained after centrifugation at 20,000 g) was determined to be 92.58 %±0.48 and 77.92 %±3.21, for 4 % and 7 % protein soymilk, respectively. This clearly indicates that the protein content relative to total solids is diminished when soymilk is prepared using a lower water-to-bean ratio. This result might have possible implications in industry. The protein subunit composition of the “supernatant after 20,000 g” samples is shown in Figure 1. Lanes 1 and 3 show the polypeptide composition of 4 and 7 % protein soymilk, respectively, while lanes 2 and 4 show the composition of the supernatant. Although the protein content of the soymilk particles was different, all the major soy protein

**Table 1** Ion composition of the ultrafiltered serums obtained from 4 % protein soymilk prepared from a water-to-soybean protein ratio of 22:1 and 7 % protein soymilk prepared from a water-to-soybean protein ratio of 12:1. Ions were analyzed by atomic absorption spectroscopy by Laboratory Services (University of Guelph, Guelph, Canada). The refractive index of serum derived from 4 % to 7 % protein soymilk is shown in the bottom row

	Serum derived from 4 % protein soymilk ( $\mu\text{g/g}$ serum)	Serum derived from 7 % protein soymilk ( $\mu\text{g/g}$ serum)
Calcium	42	77
Magnesium	110	210
Phosphorus	87	170
Potassium	940	1600
Sodium	95	95
Sulfur	57	100
Refractive Index	1.3348 <sup>a</sup>	1.3355 <sup>b</sup>

\*Values with different letters across columns are significantly different from each other.

subunits ( $\alpha$ ,  $\alpha'$ ,  $\beta$  of  $\beta$ -conglycinin and acidic and basic of glycinin) were present in the supernatant from both soymilk bases. This is in agreement with previous reports.<sup>5,7,14</sup> These experiments were repeated on the resuspended pellet (omitting the 20,000 g centrifugation step, results not shown) and the protein subunit composition obtained was similar to those shown in Figure 1.

To gain further insight into possible structural changes of the proteins present in 4 % and 7 % protein soymilk, samples were diluted to the same protein content in phosphate buffer, and subjected to fluorescence measurements. It was hypothesized that soymilk samples prepared with a different water-to-bean ratio may have a different protein structural organization.

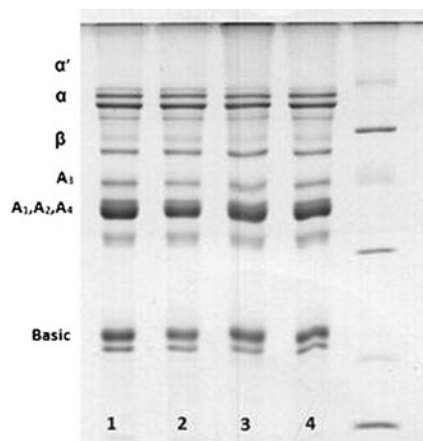


**Fig. 1** SDS-PAGE under reducing conditions of soymilk samples and their corresponding supernatant after 20,000 g (see [Materials and Methods](#)) (1) 4 % soymilk, (2) 4 % supernatant, (3) 7 % soymilk, (4) 7 % supernatant. Lane 5 shows the molecular mass markers. All samples were loaded at the same protein content of 20  $\mu\text{g}$  per well

Figure 2 illustrates the average intrinsic fluorescence spectra for the 4 and 7 % protein soymilk samples. Table 2 shows the results in terms of the wavelength of maximum intensity ( $\lambda_{\text{max}}$ ) and value of maximum fluorescence intensity ( $I_{\text{max}}$ ). Both the  $\lambda_{\text{max}}$  and the  $I_{\text{max}}$  were not significantly different from each other, which suggests high similarities between the protein structures present in both soymilk preparations. Given that previous authors<sup>4-6,13-15</sup> hypothesized that soymilk protein particles are formed through the dissociation and subsequent rearrangement of protein subunits during heating, the fluorescence results obtained suggest that the water-to-bean ratio used during extraction and heating of soymilk had no effect on the arrangement of protein particles and that soybean proteins were present in a somewhat similar conformation in soymilk. These results were further confirmed by titration using the hydrophobic probe ANS. The titration results (Table 2) confirmed the conclusions derived from intrinsic fluorescence measurements, as there were no significant differences between the affinity of the protein particles ( $K_d$  values) from 4 % to 7 % protein soymilk samples. This would suggest that different water-to-bean ratios used to prepare soymilk produced particles with similar overall surface hydrophobicity.

To determine if the size or overall charge of the soymilk particles varied with soymilk preparation conditions (water-to-bean ratios), the apparent hydrodynamic radius and the  $\zeta$ -potential were measured after dilution of the soymilk samples containing 4 and 7 % protein in buffer (for size) or their respective sera (for charge measurements). Table 3 summarizes the results, and compares the values of apparent size measured by DLS with those of apparent particle size of undiluted soymilk samples measured by diffusing wave spectroscopy (DWS). When the soymilk particles were

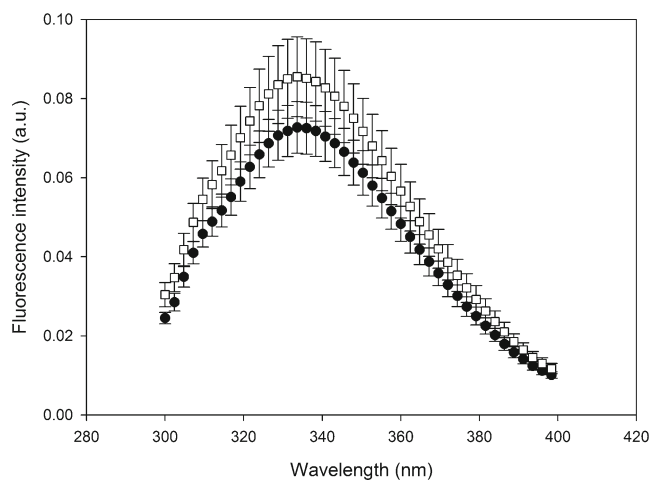


**Fig. 2** Fluorescence spectrum derived from particles of 4 % (filled circles) and 7 % (open squares) protein soymilk samples highly diluted in phosphate buffer (pH 7). Error bars represent the standard deviation from three replicates

**Table 2** Experimental values of the fluorescence spectrum and surface hydrophobicity using ANS as a probe, of diluted 4 % and 7 % soymilk samples in phosphate buffer (pH 7)

	4 % protein soymilk	7 % protein soymilk
Intrinsic Fluorescence		
$\lambda_{\max}$ (nm)	334 <sup>a</sup>	334 <sup>a</sup>
$I_{\max}$ (nm)	0.0727 <sup>a</sup>	0.0855 <sup>a</sup>
Surface Hydrophobicity		
$F_{\max}$	22092 <sup>a</sup>	19877 <sup>a</sup>
$K_d^{\text{APP}}$ ( $\mu\text{mol ANS}$ )	54.2 <sup>a</sup>	60.3 <sup>a</sup>
PSH	411 <sup>a</sup>	332 <sup>a</sup>

\*Values with different letters across columns are significantly different from each other.

measured undiluted using DWS, they appeared larger than those measured after extensive dilution in phosphate buffer (see DLS results). The discrepancy between the results of the two measurements could arise from a number of reasons. DWS and DLS have different weighting averages due to the nature of the scattering measurements. Furthermore, the high dilution of the samples (~10,000 times) necessary in DLS measurements caused changes in the mobility of the particles. It has yet to be established whether high dilution causes disruption of the soymilk particles. Finally, hydrodynamic effects due to concentration must be taken into account when dealing with concentrated samples (as those measured by DWS). The theoretical model to correct for this effect is well-known, but dependent on volume fraction. Unfortunately, there is no current knowledge of the mass-to-volume ratio of soymilk particles, and this made the transformation of protein weight into protein volume fraction not possible.

The particle size measured with both techniques showed statistically significant differences depending on the water-to-bean ratio employed in the preparation of soymilk. The DWS measurement of the undiluted 7 % protein soymilk

**Table 3** Size and  $\zeta$ -potential measurements of 4 and 7 % protein soymilk particles measured by DLS and DWS. For particle size measurements, samples measured with DWS were undiluted, while those measured with DLS were highly diluted in phosphate buffer (pH 8).  $\zeta$ -potential measurements were performed by DLS as well, and were diluted in their respective stock-derived serums

	4 % soymilk	7 % soymilk
DWS apparent particle radius (nm) (undiluted)	462.8±15.5 <sup>a</sup>	2486.3±576.0 <sup>b</sup>
DLS apparent particle radius (nm) (highly diluted in phosphate buffer)	88.8±0.79 <sup>a</sup>	180.7±30.0 <sup>b</sup>
Zeta-potential (mV)	-19.9±2.4 <sup>a</sup>	-14.1±0.5 <sup>b</sup>

\*Within a row, values with different letters across columns show statistical differences at  $p < 0.05$ .

yielded an average particle size of 2.5  $\mu\text{m}$ , in contrast to the 0.46  $\mu\text{m}$  for the 4 % protein soymilk. It was clear that protein concentration in the soymilk base had a significant impact on particle size, and maybe stability, colloidal and processing behaviour of the soymilk particles.

The value of the  $\zeta$ -potential for the 4 % protein soymilk was significantly higher than that of the 7 % protein soymilk (Table 3) however, this difference could be partially attributed to the differences in the composition of the serum phase, with the 7 % serum having higher ions in solution and therefore higher charge shielding. Nevertheless, it is important to note that both potentials were close in value and in both cases the particles were not sufficiently charged to impart full electrostatic stability.<sup>24</sup>

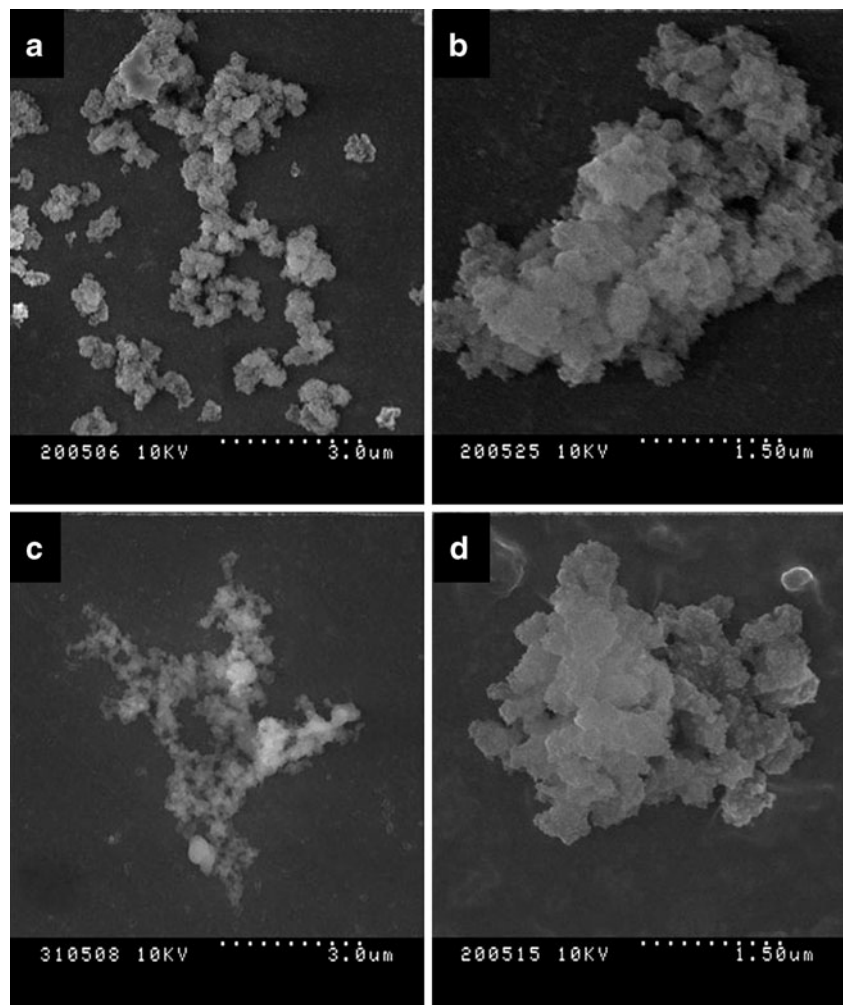
To elucidate any possible microstructural differences, SEM was carried out on the soymilk samples containing 4 and 7 % protein (Figure 3). Micrographs shown are representative of 30 and 50 micrographs captured of 4 and 7 % protein soymilk samples, respectively. The self assembled monolayer method used to prepare the samples for imaging ensured that only protein particles were covalently bound to the carbon planchet, as a rinsing step was included to remove non-protein unbound material. In addition, this method minimized possible artefacts due to surface denaturation, as it prevented direct binding to a solid surface.<sup>28</sup>

As seen in Figure 3, particles derived from different water-to-bean ratios appear to have similar aggregate-like structures, which have no overall specific shape or size, and clearly do not appear to be spherical. Although 4 % protein soymilk showed large aggregates similar to those observed in 7 % protein soymilk, the 4 % protein samples had a higher presence of small, possibly non-aggregated particles attached to the planchets. DLS results showed a high polydispersity index for both 4 % and 7 % protein soymilk, also indicating that soymilk particle size distribution is not monomodal. Particles also appeared to be much larger than the sizes reported by light scattering, for both 4 and 7 % protein soymilk samples. This was probably due to the fact that microscopy results are weighed towards the larger, more visible particles.

Cryo-TEM microscopy images of 4 % protein soymilk samples are also shown in Figure 4. Soymilk particles appear to be present as large aggregated structures (P labels), with an almost “chain-like” morphology. Some lipid globules are also visible as lighter shaded circles of about 200 nm size (L label), and they did not seem to be associated with particle aggregates. The protein aggregates seemed to be about 30 % larger when compared to sizes obtained from DWS (Table 2).

In general, it was possible to conclude that although the composition of soymilk particles (see SDS-PAGE and fluorescence measurements) may not be different between particles of soymilk made from different water-to-protein ratios, their relative protein content varied significantly; soymilk particles from 4 % protein soymilk contained

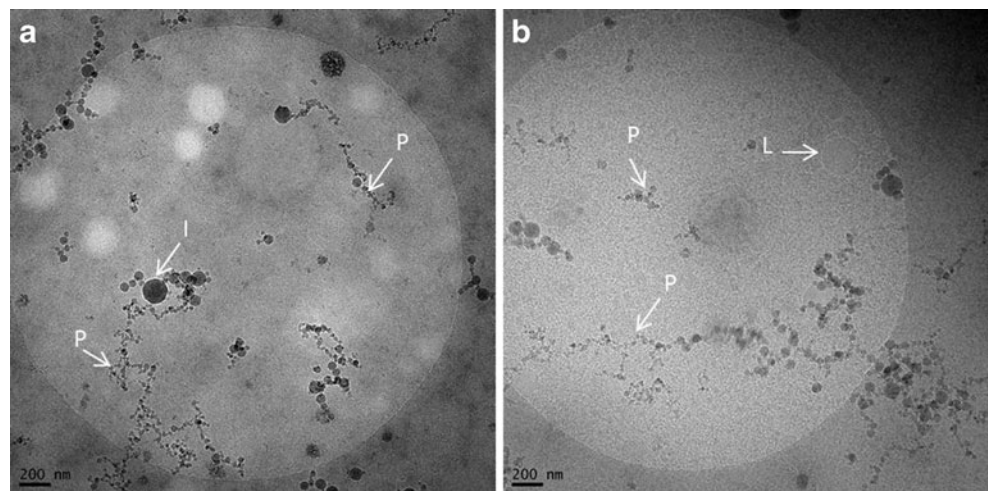
**Fig. 3** Scanning electron microscopy images of 4 % protein soymilk (**a, b**) and 7 % protein soymilk (**c, d**)



significantly more protein. In addition, light scattering measurements showed significant differences in particle sizes. The lower water-to-bean ratio produced larger particles than the more dilute soymilk base. The serum composition of these

same samples showed the same type of species, namely minerals; however the 7 % protein soymilk produced a higher number of species, which may help explain the slightly lower magnitude of  $\zeta$ -potential observed for that sample.

**Fig. 4** Cryogenic transmission electron microscopy images of 4 % protein soymilk. P: soymilk particle, I: ice crystals, L: lipids. Bar size 200 nm





The effect of protein concentration on the colloidal properties of the soymilk base is of major significance in food processing, as the aggregation state of the soymilk particles will influence their stability and processing functionality. For this reason, to better understand the colloidal behaviour of the soymilk particles prepared with different water-to-bean ratio, further experiments were performed, where the different soymilk bases (4, 5 and 7 % protein soymilk) were studied after diluting them serially in their own serum.

#### Effect of Serial Dilution on 4, 5, 7 % Protein Soymilk

Due to the seemingly direct dependence between soymilk concentration and particle size, serial dilutions of soymilk samples prepared at different initial protein concentrations were studied, 4, 5 and 7 % (w/v). It was hypothesized that soymilk particles made from a different water-to-bean ratio would behave differently when diluted, due to their apparent differences in size as observed by light scattering. Figure 5 shows the relation between total solids and protein content of the three soymilk bases, diluted in their own serum. All soymilk samples showed a linear relation between the amount of protein and the total solid content. This is in agreement with previous literature.<sup>5,29</sup> Furthermore, though the slopes of all three curves were similar, the total solids of the 7 % protein soymilk (for a given protein content) were consistently higher than those of 4 and 5 % protein soymilk. This confirms earlier findings that particles in the 7 % protein soymilk contain a lower ratio of protein to total solids (78 %) compared to the ones from 4 % protein soymilk (93 %).

Figure 6 shows the values of refractive index as a function of protein content, measured as a function of dilution from the

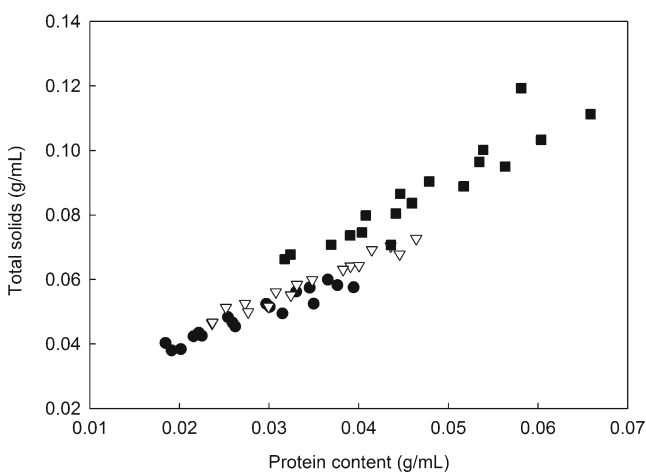


**Fig 5** Total solids content as a function of protein content of 4 % protein soymilk (filled circles), 5 % protein soymilk (open triangles) and 7 % protein soymilk (filled squares) diluted in their respective serum prepared by ultrafiltration. Data points represent single measurements of three replicates

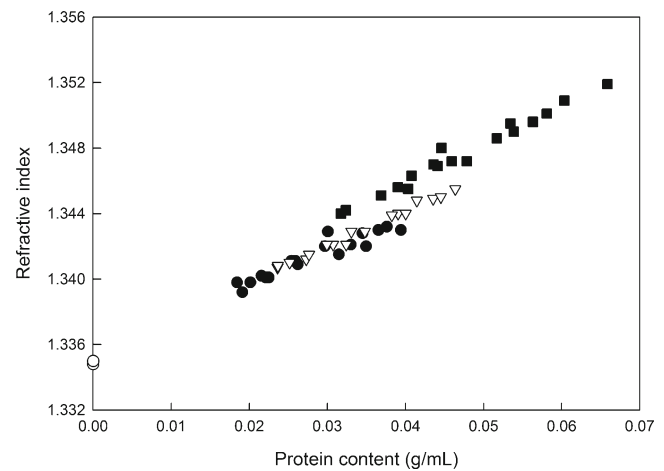


**Fig. 6** Refractive index of 4 % protein soymilk (filled circles), 5 % protein soymilk (open triangles) and 7 % protein soymilk (filled squares) diluted in their stock-derived serum. Data points represent single measurements of three replicates. Note the open circles 0 g/mL protein, corresponding to the refractive index of the serum prepared by ultrafiltration from the different soymilk samples

three soymilk bases, containing 4 %, 5 % and 7 % protein. The measured values of refractive index of the corresponding sera prepared by ultrafiltration (free of protein) are also plotted in the figure (open circles, at 0 % protein). Samples of soymilk containing 4 % and 5 % protein showed a similar trend with a linear increase of the index of refraction with increasing protein content. The refractive index values originating from the two soymilk bases at similar protein content clearly overlapped, consistent with the notion that the amount of matter present in the system drives the change in refractive index values. Also, and as reported in Table 1, the refractive index of the serum phase was close to that of water, indicating that the change in the effective refractive index of soymilk was mainly caused by the dispersed phase, and thus was proportional to the protein concentration in the soymilk.

Consistent with the results of total solids (Figure 5), the values of refractive index for the dilutions of the 7 % protein soymilk also lay well above those of the other two soymilk samples, even in the overlap region where the protein concentration of the soymilk samples was equal. Since the nature and origin of the particles was similar (see above), and the refractive index of the serum itself (Table 1) could not account for such difference, it is possible to hypothesize that the higher refractive index in the soymilk base prepared with less water indicated the presence of denser particles (i.e. less hydrated) than in the soymilk base prepared with 4 or 5 % protein. It is also possible to assume that the refractive index differences could be partly due to the different nature of the particles as the protein-to-solids ratio in the 7 % soymilk base samples was lower.

The changes in the optical properties of the soymilk particles as a function of concentration were determined using DWS. Figure 7 shows the changes in turbidity (A)

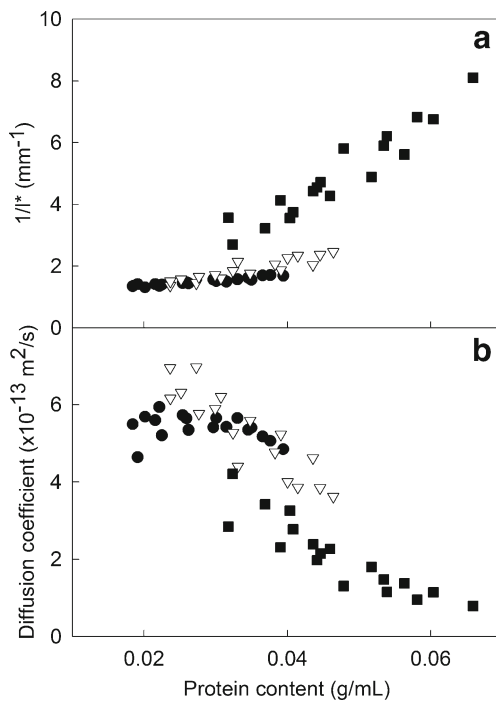


**Fig. 7** DWS results of (a) photon transport mean free path,  $1/l^*$ , and (b) diffusion coefficient of 4 % protein soymilk (filled circles), 5 % protein soymilk (open triangles) and 7 % protein soymilk (filled squares) diluted in their stock-derived serum. Data points represent single measurements of three replicates

and diffusion coefficient (B), for the 4, 5 and 7 % protein soymilk, all diluted in their respective sera. The behaviour of the turbidity parameter ( $1/l^*$ ) showed two fairly distinct regions (Figure 7a). The soymilk particles in 4 % and 5 % protein soymilk yielded similar  $1/l^*$  values as a function of dilution, while the  $1/l^*$  parameter for the 7 % protein soymilk particles was well above the others, and showed a different dependence with concentration (with a higher slope). In general, the turbidity for the soymilk bases containing 4 % and 5 % protein increased in value in the range between 0.03 mg/mL and 0.045 mg/mL protein (this difference was statistically significant for  $p < 0.05$ ). The increase in the  $1/l^*$  value reflects the fact that, as the system became more concentrated, more scattering events occur in the same scattering volume resulting in shorter decorrelation lengths. While the soymilk base samples with 4 and 5 % protein showed the same behaviour as a function of concentration of protein, the soymilk base prepared with 7 % protein diverged noticeably. It could be possible to calculate the expected behaviour of turbidity from theory for a colloidal hard-sphere model<sup>23</sup> and compare this to the bulk behaviour of soymilk particles; however, this would require knowledge of the volume fraction occupied by the particles which is not currently known.

Using DWS it was also possible to determine changes in the mobility of the particles (diffusion coefficient) as a function of their protein concentration (Figure 7b). Overall, the

diffusion coefficient decreased with increasing protein concentration. In agreement with the turbidity data, the soymilk particles in the 4 and 5 % protein soymilk base showed similar particle diffusion behaviour, while those in the 7 % protein soymilk base showed a rather dramatic decrease in the diffusion coefficient, both at the high protein concentrations and even when diluted to the same protein content as the 4 and 5 % protein base samples. The soymilk particles prepared from the high protein (7 %) base had a much lower diffusion coefficient compared to the particles prepared from 4 % and 5 % protein soymilk. This could be a product of the differences in protein content and hence optical properties of the soymilk particles, as discussed earlier.

It is important to note at this time, that the correlation functions from which these data were extracted showed free-diffusing motion of the particles and therefore, these are true short-time self-diffusion values for the particles present in the various soymilk bases. However, the values of diffusion coefficient have not been corrected for crowding effects, and, given the high protein contents of samples investigated in this work, this might play an important role in determining differences in self diffusion values. The dynamic behaviour of the soymilk particles could also be compared to the Beenakker–Mazur<sup>30</sup> calculations of the theoretical, normalized self-diffusion coefficient for hard spheres; however these calculations necessitate knowledge of volume fraction, and as explained above, no previous reports on the volume occupied by a soymilk particle in soymilk are available in the literature.

The effect of protein concentration of the bulk viscosity of the different soymilk bases can also give indications of the colloidal behaviour of the soymilk particles. Results of viscosity measurements of diluted soymilk (Figure 8) show

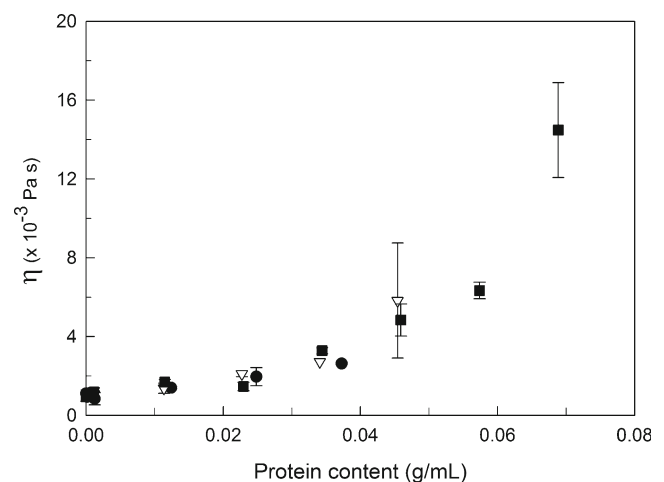


**Fig. 8** Viscosity of soymilk samples measured at  $100 \text{ s}^{-1}$  for 4 % protein soymilk (filled circles), 5 % protein soymilk (open triangles) and 7 % protein soymilk (filled squares) diluted in water. Data points represent single measurements of three replicates

that, under steady flow conditions, the viscosity increased with increasing concentration of the particles in solution. This is expected, and is in agreement with previous work.<sup>31</sup> Unlike the light scattering measurements, the changes of viscosity with protein concentration were independent of the protein concentration of the original stock solution, as all the results superimposed on one another. This is important, as it may suggest a shear dependence of the colloidal state of the particles, as this was not the case for quiescent light scattering measurements (see Figure 7). The shape of the curve is reminiscent of those obtained for other colloidal systems, such as for example, milk.<sup>32</sup> In the case of the dependence of viscosity with concentration in milk, the semi-empirical model known as the Eilers model<sup>33</sup> is able to reproduce and predict the viscosity behaviour of fresh skim bovine milk as a function of the volume fraction. However, knowledge of the volume occupied by the particles would be necessary to apply any models to predict the behaviour of soymilk particles and, as already mentioned, this is not known at the moment.

#### Comparison of Experimental Data with Theoretical Models

As mentioned above, the interpretation of the behaviour of the soymilk particles in terms of theoretical models requires the conversion of mass-to-volume of the soymilk protein particles. Such conversion is currently unknown and not available in literature. For this reason, the factor (sometimes known as voluminosity) by which the particle mass can be translated to volume, was derived from an evaluation of the experimental data obtained from independent methods. This allowed for interpretation of the general bulk property behaviour of soymilk particles in solution, and a comparison of this behaviour with those of well-known colloidal systems.

In view of the different protein-to-solid content ratio of particles in the 7 % soymilk, as well as the different concentration dependence of refractive index, turbidity and diffusivity, it was decided to focus on the data derived from 4 % and 5 % protein soymilk alone.

The initial calculations were taken from the refractive index results shown in Figure 6. It is known that the index of refraction of a dispersion can be written as a relation between the refractive index of the solvent and of the solute, using a suitable “mixture rule” as follows<sup>34</sup>:

$$n_{\text{exp}}^2 = n_{\text{particle}}^2(\phi_{\text{particle}}) + n_{\text{serum}}^2(\phi_{\text{serum}}) \quad (4)$$

where  $n_{\text{exp}}$  is the experimentally-obtained index of refraction of the colloidal mixture,  $n_{\text{serum}}=1.3352$  and  $n_{\text{particle}}$  are the indices of refraction of the serum and soymilk particles respectively, and  $\phi_{\text{serum}}$  and  $\phi_{\text{particle}}$  are their respective volume fractions. The volume fraction of the particles is

simply the concentration of protein (in mass/volume) multiplied by a constant parameter (usually called “voluminosity”,  $V$ ). Knowing all this, Equation 4 can be re-written as:

$$n_{\text{exp}}^2 = n_{\text{particle}}^2(V C_{\text{particle}}) + n_{\text{serum}}^2(1 - V C_{\text{particle}}) \quad (5)$$

where  $C_{\text{particle}}$  is the protein content of the solution (in g/mL) and  $V$  is the voluminosity of the soymilk particles (in mL/g). The factor  $(1 - V C_{\text{particle}})$  represents the space occupied by the serum (space unoccupied by the particles) and it is, therefore, the volume fraction corresponding to the serum phase.

Equation 4 has two unknown parameters ( $n_{\text{particle}}$  and the voluminosity, parameter  $V$ ). There are, therefore, infinite numbers of paired values that satisfy the conditions given by this equation. However, for a given index of refraction of the particles, there is one, and only one, possible associated volume fraction. This pair-solution would be of critical importance for the calculations below.

There is a second possible theoretical model fit that can be performed on the turbidity data which were collected by DWS. It is that shown in Equation 2 for the  $1/l^*$  results shown in Figure 7. In order to solve this equation, several input values are needed, such as: the refractive index of the serum as well as the size, refractive index and volume fraction of the particles. As clearly concluded above, the refractive index and volume fraction of the particles are still unknown at this point, however, and most importantly, they are now paired and unequivocally related by means of the fit to Equation 5. Therefore, for a given paired value generated by this equation, the parameter  $V$  was multiplied by the protein content to generate the volume fraction of the particles needed for Equation 2, and the corresponding  $n_{\text{particle}}$  generated by the fit was also used as input in the equation.

A theoretical curve for  $1/l^*$  was then generated for a colloidal hard-sphere model, applying the Percus–Yevick closure relation<sup>35</sup> for the calculation of the structure factor  $S(q)$  coupled with Mie calculations for the scattering function  $F(q)$ . The other experimental parameters used were  $n_{\text{serum}}=1.3352$  (obtained from the best-fit line of the curves shown in Figure 6) and particle size  $R_{\text{particle}}=0.425 \mu\text{m}$  (obtained by averaging the first 25 points of Figure 7b and converting the diffusion coefficients to radii by means of the Stokes–Einstein equation. Numerous pairs were tested using Equation 4 until the best fit to the values shown in Figure 7a was obtained. The results of this fit are shown in Figure 9a (solid line), plotted as the  $1/l^*$  parameter as a function of volume fraction of soymilk particles in solution. The data is the same as those shown in Figure 7a (but plotted against volume fraction this time). The best-fit parameters obtained were  $n_{\text{particle}}=1.388$  with a  $V$  value of 4.11 mL/g. The lower and upper limits were calculated as  $n_{\text{particle}}=1.383$  and 1.392 and  $V=4.55$  and 3.81 mL/g, respectively (dotted lines).

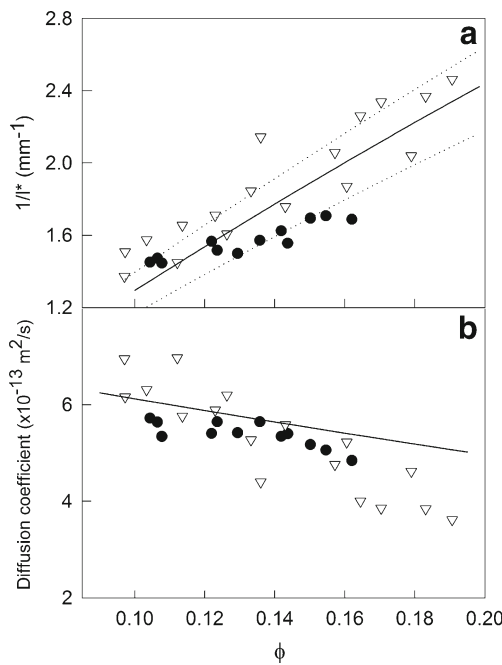


**Fig. 9** DWS results of (a) photon transport mean free path,  $1/l^*$ , and (b) diffusion coefficient of 4 % protein soymilk (filled circles), 5 % protein soymilk (open triangles) plotted as a function of volume fraction. Data points represent single measurements of three replicates. The solid lines represents the theoretical  $1/l^*$  values calculated with a particle refractive index of  $n_{\text{particle}}=1.388$  and a voluminosity  $V$  value of 4.11 mL/g and a constant  $R_{\text{particle}}=0.425 \mu\text{m}$

These results are extremely interesting on three accounts. First, by employing two independent and different measuring methods (refractometry and DWS) it was possible to find a set of solutions which satisfied both model systems. Secondly, soymilk particles in bulk seem to follow the overall bulk behaviour of model, monodisperse spheres. The fit seen in Figure 9a is relatively good considering the complexity of the soymilk and the far-from-model system of soymilk particles, particularly considering a sphere-equivalent value was used for size, knowing that soymilk particles are far from spherical (as shown in the microscopy data). Thirdly, the values obtained for refractive index and voluminosities of the particles are comparable to those of other well known colloidal protein particles, for example, casein micelles in milk ( $RI_{\text{micelle}}=1.39\text{--}1.40$  and voluminosity=3.5–4.5 mL/g).<sup>36,37</sup> It is known that casein micelles are highly hydrated structures, while soy proteins are thought to be globular and less hydrated. The microscopy data showed that soy particles indeed are not spherical, and so the high degree of particle hydration could be partially attributed to the sphere-equivalent assumption used in our calculations. Also noteworthy is the fact that all the data obtained from the two different stock solutions, namely 4 % and 5 % soymilk, could be fitted using a constant value of the radius.

Figure 9b shows the normalized diffusion coefficients (same data as Figure 7b) also plotted as a function of volume fraction. Superimposed is the normalized self-diffusion coefficient for hard spheres of constant size, calculated using the Beenakker–Mazur formulation.<sup>30</sup> This formulation calculates the diffusion coefficient of particles assumed to be hard spheres and mathematically incorporates the effect of hydrodynamic forces exerted between two particles when in close proximity (at high volume fractions). The normalization was performed assuming that a chosen soymilk particle at 10 % volume fraction followed the hard sphere model theory. From this graph it becomes clear that, dynamically, the soymilk particles derived from the 4 and 5 % protein base did not follow the behaviour of perfect hard spheres above a volume fraction of about 15 %, since the experimental values deviated from theory. This behaviour tends to indicate that at a given volume fraction, the diffusion coefficient measured by DWS was lower than that of theory, suggesting that the particles “dragged” more in solution (move more slowly) at the higher volume fractions. It is not clear at this moment what the origin of this deviation is, although the microscopy images shown in Figures 3 and 4 may suggest that it could be due to the “chain-like” morphology of the soymilk particles. The diffusion of the soymilk particles could be mimicked using a sphere-equivalent radius only in the very dilute region of the system. The values of diffusion coefficient of 7 % protein soymilk particles were much smaller than those for 4 and 5 % protein soymilk (see Figure 7b), and hence deviated from theory even more.

Making use of the ability to fit experimental data as a function of volume fraction,  $\phi$ , the viscosity values shown in Figure 8 could also be compared to theory. Recently, a model was derived for the calculation of viscosities of concentrated suspensions taking into account both hydrodynamic and excluded-volume effects. This model extends the viscosity-concentration relation not only for spherical particles, but also for other particle shapes (given they are not too elongated).<sup>38</sup> The relation is shown in Equation 6:

$$\eta(\phi) = \eta_o \left[ 1 - \left( \frac{\phi}{1 - c\phi} \right) \right]^{-[\eta]} \tag{6}$$

where  $\eta_o$  is the viscosity of the system at 0 shear,  $[\eta]$  is the low-filling fraction intrinsic viscosity of the system and  $c$  is the crowding factor defined as

$$c = \frac{1 - \phi_c}{\phi_c} \tag{7}$$

This factor takes into account the fact that the particles cannot occupy 100 % of the volume of the system due to geometrical restrictions. The value of the intrinsic viscosity,  $\eta$ , has been theoretically determined for a large number of geometries<sup>39</sup> and can have values ranging between 2.5 and 30 or more (a value of 2.5 was obtained by Einstein<sup>39</sup> for



spherical uncharged particles). The value of  $\phi_c$ , on the other hand, has been calculated as  $\sim 0.65$  for random close-packing of spheres, but can also have different values depending on the geometry of the filling particles (Figure 10).

The solid line in Figure 11 shows the best-fit curve to the experimental values. The resulting values for this fit were  $\phi_c = 0.58$  and  $[\eta] = 6.1$ . Similar calculations performed for ellipsoids, which assume a length four times their width, yielded values of  $\phi_c = 0.53$  and  $[\eta] = 5.3$ . It would be premature to conclude from this fit that soymilk particles are shaped as such (ellipsoid), especially due to the polydispersity of particle size and many-component nature of the system; however, obtaining such extremely acceptable fits which yielded values similar to a model system, is highly reassuring. It is important at this point to clarify that the parameters obtained in this fit, which are relatively consistent with those of an ellipsoid, are not in conflict with those obtained for a sphere-like system for the turbidity (Figure 9a). The viscosity models are independent of size, and it is always possible to find a sphere-like radius for any given geometrical shape.

The normalized dynamic electrophoretic mobility of soymilk particles collected from electroacoustic spectroscopy measurement was also plotted as a function of the newly derived volume fraction, along with the dynamic mobility of Ludox silica spheres, in Figure 11.

Equation 3 relates the ultrasound CVI with the electrophoretic mobility via density and surface conductivity (through  $F(Z)$ ) of the particles. Unfortunately, these are unknown parameters in soymilk but furthermore, the dependence (if any) between them and volume fraction is also unknown. On the other hand, it is well known that silica particles are a hard sphere model system of constant density and surface charge as a function of concentration.<sup>24</sup> For this reason, the behaviour of the soymilk mobility could be directly compared to the Ludox behaviour (albeit via a normalization factor).

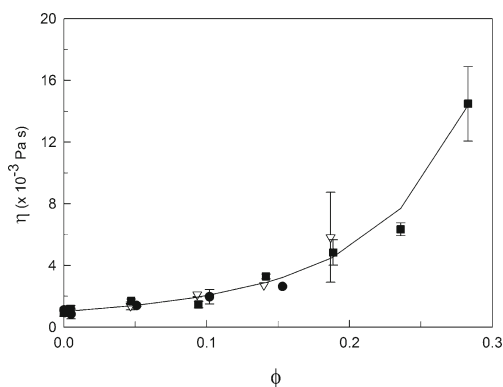


**Fig. 10** Viscosity measured at  $100 \text{ s}^{-1}$  of 4 % (filled circles), 5 % (open triangles) and 7 % (filled squares) protein soymilk samples and plotted as a function of volume fraction. Superimposed are the theoretical lines generated using the Mendoza (solid) model

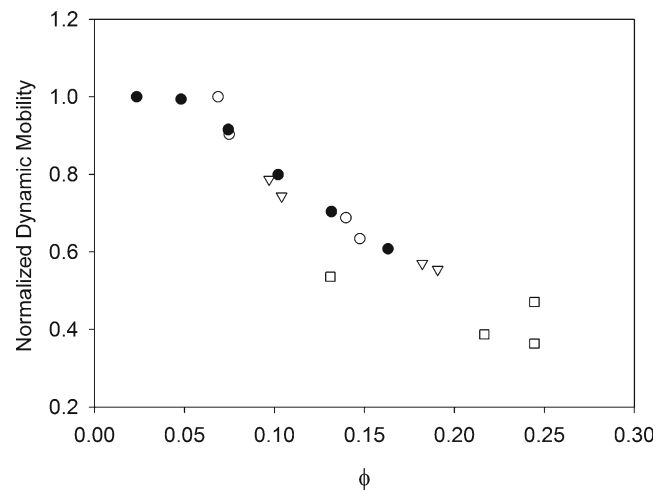


**Fig. 11** Normalized dynamic electrophoretic mobility of soymilk particles measured by electro-acoustic spectroscopy for 4 % protein soymilk (open circles), 5 % protein soymilk (open triangles) and 7 % protein soymilk (open squares) diluted in their stock-derived serum. Data points represent single measurements of three replicates. The dynamic mobility of a ludox silica sphere suspension is also shown (filled circles)

The normalized dynamic mobility as a function of volume fraction showed a similar behaviour between the Ludox (hard spheres) silica particles and soymilk particles. There was a decrease of electrophoretic mobility as a function of volume fraction. The viscosity of the background of both systems (soymilk and Ludox silica sphere suspension) was assumed to be equivalent to water. It is important to note that also in this case, soymilk particles derived from 7 % protein soymilk (open squares) showed a different behaviour compared to 4 and 5 % protein soymilk.

With the measurements carried out by electroacoustics (Figure 11), further conclusions can be made on the soymilk particles. Given that the soymilk particles showed a very similar behaviour to Ludox spheres, and that these standard particles have constant density throughout the experimental volume fractions probed, it can be concluded that the density was also constant for the soymilk colloids. These results are of great importance, and have never been reported before. Furthermore, the data shown in Figure 11 also suggest that the surface charge of the soymilk particles did not change as a function of concentration. Unfortunately, the need to normalize for comparison did not allow for the determination of an absolute density of the particles, thereby making it impossible to corroborate the voluminosity value obtained from DWS. Nevertheless, these results reinforce the validity of the particle voluminosity factor derived from this study, since the dependence of dynamic mobility on volume fraction for the soymilk particles matched that of the model systems (Ludox spheres).

## Conclusions

Soy milk was prepared from different water-to-bean ratios to investigate how the protein concentration of the soy milk base would affect various physical parameters of soy milk particles and soy milk as a bulk. The composition of soy milk particles was similar in subunit composition, but varied significantly in protein content. Fluorescence spectroscopy measurements suggested that similar rearrangements of subunits occurred in all soy milk particles, independently on the original protein concentration in the soy milk base. When the optical characteristics of soy milk were investigated further by means of DWS and refractometry, it was clear that both 4 % and 5 % protein soy milk samples behaved similarly, while the 7 % protein soy milk showed deviations which may be linked to a lower hydration of the particles and difference in protein-to-solid content ratio. It was therefore concluded that when using different ratios of water-to-bean, caution should be used, as different soy milk particles could be obtained, with obvious consequences to processing functionality of the soy milk base.

To interpret the data obtained from turbidity, size, viscosity measurements and dynamic mobility of the soy milk samples as a function of theoretical models, it was necessary to calculate the voluminosity of soy milk particles. This value (4.11 mL/g) was derived, for the first time, from independent experimental data. The determination of such an important parameter made it possible to find a satisfactory theoretical fit for the turbidity ( $1/l^*$ ) parameter and to obtain an index of refraction of the soy milk particle of 1.388. These values suggested that soy milk particles maybe somewhat more hydrated, in contrast to what is normally believed of globular proteins.

Taking into consideration the lack of homogeneity of the particle size distribution, the deviation from sphericity and the presence of extraneous material in solution, it is quite noteworthy that based on hard-sphere analogy only, it was possible to quantitatively calculate the optical properties of the soy milk particles. Furthermore, the results showed that soy milk particles create more hydrodynamic drag than those of a hard sphere system, indication of the lack of the sphericity of the particles. These results were further confirmed with the drastic increase in viscosity at volume fractions much smaller than those predicted for hard spheres, as fitting parameters were closer to those of ellipsoids. The dependence of dynamic mobility measured by electroacoustics with volume fraction also lead to the conclusion that the density and surface charge of the soy milk particles was constant up to 25 % volume fractions, and gave further validity to the voluminosity found by DWS.

The new information presented in this work opens the door for future comparisons of experimentally-obtained results to various theoretical models.

## References

1. C.R. Sirtori, R. Even, M.R. Lovati, *Ann New York Acad Sci* **676**, 201 (1993)
2. M.J. Messina, V. Persky, K.D.R. Setchell, S. Barnes, *Nutr Canc* **21**, 113 (1994)
3. K.D.R. Setchell, *Asia Pac J Clin Nutr* **9**, 13 (2001)
4. R. Lakshmanan, M. De Lamballerie, S. Jung, *J. Food Sci.* **71**, E384 (2006)
5. A. Malaki Nik, S. Tosh, V. Poysa, L. Woodrow, M. Corredig, *Food Res Int* **41**, 286 (2008)
6. M. Shimoyamada, N. Tsushima, K. Tsuzuki, H. Asao, R. Yamauchi, *Food Sci Technol Res* **14**, 32 (2008)
7. C. Ren, L. Tang, M. Zhang, S. Guo, *J. Agric. Food Chem.* **57**, 1921 (2009)
8. K.C. Kwok, K. Niranjana, *Int. J. Food Sci. Tech.* **30**, 263 (1995)
9. K. Liu, *Soybeans: Chemistry, Technology, and Utilization* (Chapman and Hall, New York, 1997)
10. K.C. Kwok, H.H. Liang, K. Niranjana, *J Agric Food Chem* **50**, 4834 (2002)
11. C.I. Iwuoha, K.E. Umunnakwe, *Food Chem.* **59**, 373 (1997)
12. S. Damodaran, J.E. Kinsella, *J. Agric. Food Chem.* **30**, 812 (1982)
13. S. Utsumi, S. Damodaran, J.E. Kinsella, *J. Agric. Food Chem.* **32**, 1406 (1984)
14. T. Ono, M.R. Choi, A. Ikeda, S. Odagiri, *Agric Biol Chem* **55**, 2291 (1991)
15. T. Ono, S. Katho, K. Mothizuki, *Biosci Biotech Biochem* **57**, 24 (1993)
16. S.T. Guo, T. Ono, *J. Food Sci.* **70**, C258 (2005)
17. S.T. Guo, T. Ono, M. Mikami, *J. Agric. Food Chem.* **45**, 4601 (1997)
18. H. Zhang, L. Li, E. Tatsumi, S. Isobe, *Lebensmittel-Wissenschaft Und-Technologie* **38**, 7 (2005)
19. N. Cruz, M. Capellas, M. Hernandez, A.J. Trujillo, B. Guamis, V. Ferragut, *Food Res. Int.* **40**, 725 (2007)
20. L. Sivanandan, R.T. Toledo, R.K. Singh, *Int J Food Prop* **13**, 580 (2010)
21. A. Moro, C. Gatti, N. Delorenzi, *J Agric. Food Chem.* **49**, 4784 (2001)
22. M. Alexander, D.G. Dalgleish, *Colloid Surface B* **38**, 83 (2004)
23. D.A. Weitz, J.X. Zhu, D.J. Durian, H. Gang, D.J. Pine, *Phys. Scripta* **49**, 610 (1993)
24. A.S. Dukhin, P.J. Goetz, *Ultrasound for characterizing colloids*, 1st edn. (Elsevier, Amsterdam, 2002)
25. R.W. O'Brien, A. Jones, W.N. Rowlands, *Colloid Surface A: Physicochem Eng Aspect* **218**, 89 (2003)
26. V.I. Uricanu, M.H.G. Duits, J. Mellema, *Langmuir* **20**, 5079 (2004)
27. A.H. Martin, H.D. Goff, A. Smith, D.G. Dalgleish, *Food Hydrocoll.* **20**, 817 (2006)
28. K. Wadu-Mesthrige, N.A. Amro, G.Y. Liu, *Scanning* **22**, 380 (2000)
29. S. Min, Y. Yu, S.S. Martin, *J. Food Sci.* **70**, C8 (2005)
30. C.W.J. Beenakker, P. Mazur, *Phys A Stat Theor Phys* **120**, 388 (1983)
31. L.L. Forster, L.K. Ferrier, *J. Food Sci.* **44**, 583 (1979)
32. M.C.A. Griffin, J.C. Price, W.G. Griffin, *J Colloid Interf Sci* **128**, 223 (1989)
33. V.H. Eiler, *Kolloid-Z.* **97**, 313 (1941)
34. W. Heller, *J. Chem. Phys.* **69**, 1123 (1965)
35. J. Hansen, I. McDonald, *Theory of Simple Liquids*, 2nd edn. (Academi, London, UK, 1986)
36. C. Holt, D.W.L. Hukins, *Int. Dairy J.* **1**, 151 (1991)
37. M. Alexander, L.F. Rojas-Ochoa, M. Leser, P. Schurtenberger, *J. Colloid Interface Sci.* **253**, 35 (2002)
38. C.I. Mendoza, I. Santamaria-Holek, *J. Chem. Phys.* **130**, 044904 (2009)
39. A. Einstein, *Investigations on the Theory of the Brownian Movement*, (Dover Pubns, 1956)